Nature of Adhesion of Condensed Organic Films on Platinum by First-Principles Simulations (Supplementary Information)

Slimane Laref,[a] Yan Li[a], Marie-Laure Bocquet[a], Françoise Delbecq[a], Philippe Sautet[a] and David Loffreda*[a]‡

Received 26th October 2010
DOI: 10.1039/b000000x

1 Solid Organic-Metal Interfaces

1.1 Interface Structures

The optimal structures (minimized densities) of the solid organic-metal interfaces are exposed in Fig. 1. The number of interfacial molecules can be easily seen in these stereographic views: 16 interface CC_4 molecules on (a) and 8 interface ethanol molecules on (b). For CC_4/Pt(111), the most stable structure (final state FS) is shown. At the metal surface, one CC_4 molecule is completely dissociated giving a di-σ(C-Cl) $CCl_{3,ads}$ + bridge Cl_{ads} coadsorption structure. For ethanol/Pt(111), four ethanol molecules are adsorbed (both sides of the metallic slab) and four other ones are physisorbed.

1.2 Interface tension and interface energy decomposition

The interface tension $\Gamma_{interface}$ can be decomposed following the scheme presented in Fig. 2 and the equations derived hereafter. $\Gamma_{interface}$ is easily calculated from the total electronic energies of the interface model and the references of the solid (liquid) organic crystal (bulk) and the platinum bulk (see Eq. (1) and Fig. 2). It can be decomposed into three contributions: the surface energy of the organic surface γ^{mol}_{surf}, the surface tension of the clean Pt(111) surface γ^{met}_{surf} and the adhesion surface energy γ_{adh}. Each of three components is defined is Eq. (3), (4) and (5), respectively.

The adhesion energy E_{adh} can also be decomposed into three contributions according to Eq. (6): the interaction energy between the organic phase and the metal in the geometry of the interface $E^{mol/met}_{interac}$, the deformation energy of the organic surface between the relaxed natural surface (monoclinic phase) and the interface E^{mol}_{def} and the deformation energy of the Pt(111) between the relaxed isolated surface and the interface E^{met}_{def}. This last expression is thus similar with the one classically used for the decomposition of the adsorption energy of one molecule at a gas/metal interface,[1] except for the reference of the deformation energy of the adsorbate (gas phase isolated molecule).

The interaction energy $E^{mol/met}_{interac}$ is easily calculated from Eq. (7) with the total electronic energy of the interface $E^{N_{sol}}_{sol/Pt}$ and the total electronic energies of the separated partners in the geometry of the interface $E^{N_{sol}}_{frozen\ surf\ fcc}$ and $E^{N_{Pt}}_{frozen\ Pt111}$. The expressions for calculating the deformation energies are also given in Eqs. (8) to (11).

$$\Gamma_{interface} = \frac{E^{N_{sol}}_{sol/Pt} - (E^{N_{sol}}_{sol} + N_{Pt} \times E^{Pt}_{bulk})}{2A} \quad (1)$$

$$\Gamma_{interface} = \gamma^{mol}_{surf} + \gamma^{met}_{surf} + \gamma_{adh} \quad (2)$$

$$2A \times \gamma^{mol}_{surf} = E^{N_{sol}}_{surf} - E^{N_{sol}}_{sol} \quad (3)$$

$$2A \times \gamma^{met}_{surf} = E^{N_{Pt}}_{relaxed\ Pt111} - N_{Pt} \times E^{Pt}_{bulk} \quad (4)$$

$$2A \times \gamma_{adh} = E_{adh} = E^{N_{sol}}_{sol/Pt} - (E^{N_{sol}}_{surf\ monocl} + E^{N_{Pt}}_{relaxed\ Pt111}) \quad (5)$$

$$E_{adh} = E^{mol/met}_{interac} + E^{mol}_{def} + E^{met}_{def} \quad (6)$$

$$E^{mol/met}_{interac} = E^{N_{sol}}_{sol/Pt} - (E^{N_{sol}}_{frozen\ surf\ fcc} + E^{N_{Pt}}_{frozen\ Pt111}) \quad (7)$$

$$E^{mol}_{def} = E^{mol}_{trans} + E^{mol}_{relax} = E^{N_{sol}}_{frozen\ surf\ fcc} - E^{N_{sol}}_{surf\ monocl} \quad (8)$$

$$E^{mol}_{trans} = E^{N_{sol}}_{surf\ fcc} - E^{N_{sol}}_{surf\ monocl} \quad (9)$$

$$E^{mol}_{relax} = E^{N_{sol}}_{frozen\ surf\ fcc} - E^{N_{sol}}_{surf\ fcc} \quad (10)$$

$$E^{met}_{def} = E^{N_{Pt}}_{frozen\ Pt111} - E^{N_{Pt}}_{relaxed\ Pt111} \quad (11)$$

In Table 1, these energetic contributions are all listed for both solid CCl_4 and ethanol/Pt(111) systems. For CCl_4/Pt(111), the results of the three possible states (molecular state MS, immediate dissociated state DS and final state FS) appearing along the dissociation pathway of one CCl_4 molecule are given.

[a] *Université de Lyon, CNRS, Ecole Normale Supérieure de Lyon, Institut de Chimie de Lyon, Laboratoire de Chimie, 46 Allée d'Italie, F-69364 Lyon Cedex 07, France.*
‡ Corresponding author: Fax: +33.4.72.72.88.60; Tel: +33.4.72.72.88.43; E-mail: David.Loffreda@ens-lyon.fr.

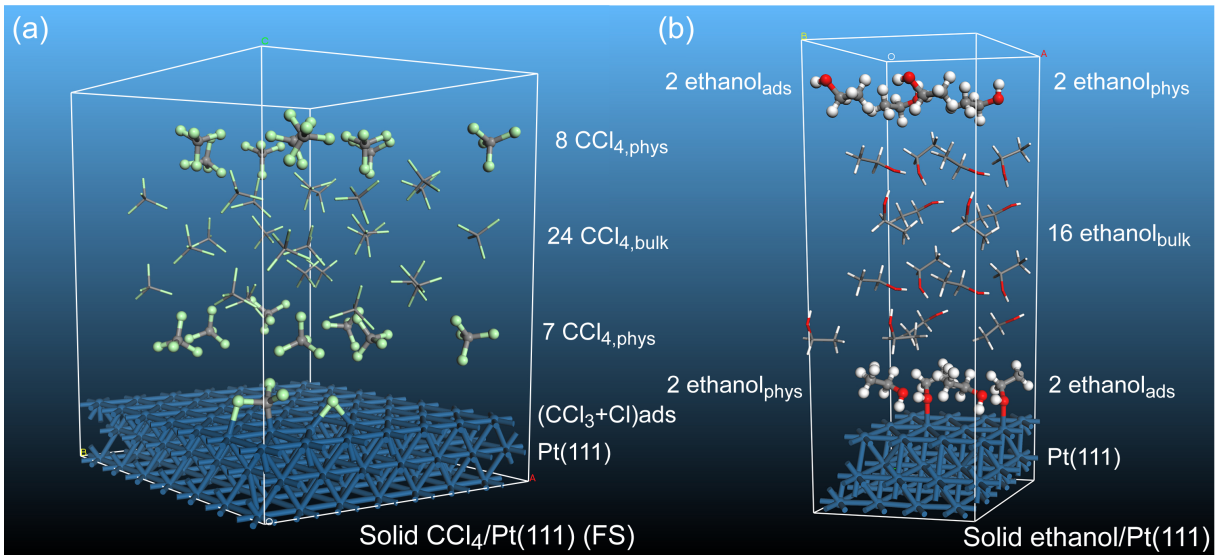

Fig. 1 Stereographic views of the optimized structures of the solid (a) CCl_4/Pt(111) (final state FS) and (b) ethanol/Pt(111) interfaces. The represented 3D boxes are related to the unit cells of the respective (7×7) and (4×3) supercells. The interface is composed of 40 CCl_4 (24 ethanol) molecules and 147 (36) platinum atoms (three metallic layers), respectively. On (a) the CCl_4 solid phase is composed of one CCl_4 dissociated molecule at the Pt(111) surface (di-σ(C-Cl) $CCl_{3,ads}$ + bridge Cl_{ads}), 15 $CCl_{4,phys}$ physisorbed molecules (ball and stick representation) and 24 $CCl_{4,bulk}$ bulk molecules (stick representation). On (b) the ethanol solid phase is composed of four ethanol adsorbed molecule at the Pt(111) surface (ethanol$_{ads}$), 4 ethanol$_{phys}$ physisorbed molecules (ball and stick representation) and 16 ethanol$_{bulk}$ bulk molecules (stick representation).

Table 1 Decomposition of the interface tension $\Gamma_{interface}$ and the adhesion energy E_{adh} following Fig. 2.

	CCl_4/Pt(111)			ethanol/Pt(111)
	MS	DS	FS	
$\Gamma_{interface}$ (J·m^{-2})	1.58	1.59	1.55	1.76
γ^{mol}_{surf} (J·m^{-2})	0.06	0.06	0.06	0.18
γ^{met}_{surf} (J·m^{-2})	1.52	1.52	1.52	1.52
γ_{adh} (J·m^{-2})	-0.00	0.01	-0.03	0.05
E_{adh} (kJ·mol^{-1})	-4	11	-139	47
E^{mol}_{trans} (kJ·mol^{-1})	80	80	80	140
E^{mol}_{relax} (kJ·mol^{-1})	6	170	340	127
E^{mol}_{def} (kJ·mol^{-1})	86	251	420	266
E^{met}_{def} (kJ·mol^{-1})	0	6	33	8
$E^{mol/met}_{interac}$ (kJ·mol^{-1})	-91	-245	-593	-227

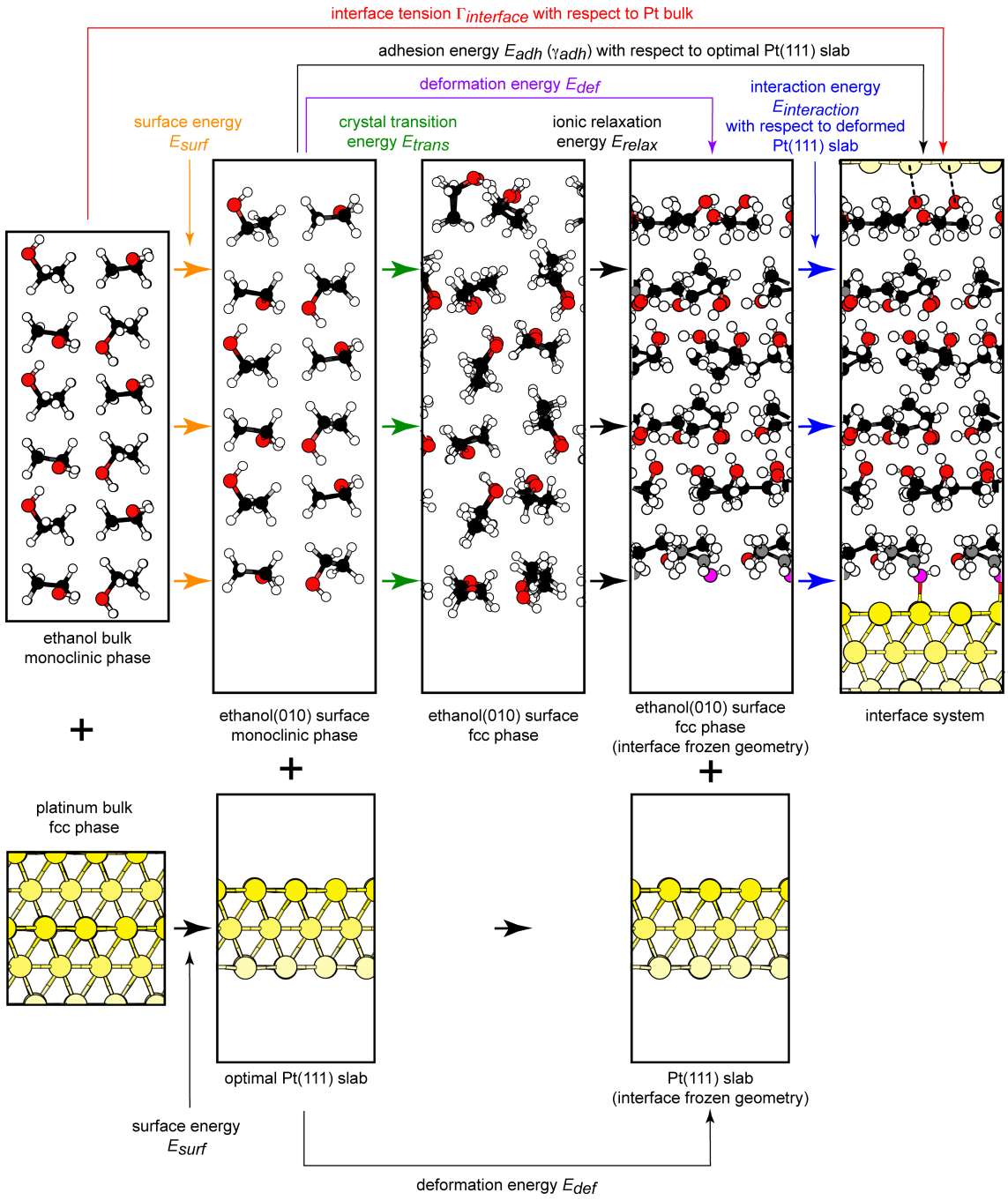

Fig. 2 Energy decomposition model for the solid organic-metal interfaces. The interface tension $\Gamma_{interface}$ (J.m^{-2}) is calculated from the total electronic energy of the bulk materials (organic crystal and platinum). The formation and relaxation of the (010) surface from the monoclinic phase of the organic crystal requires a surface energy noted E_{surf}. The change of crystallinity for the relaxed (010) organic surface from monoclinic to fcc phases can be defined as the crystal transition energy E_{trans}. The change of geometry for the organic molecules between the relaxed structure of the (010) surface in the fcc phase and the situation in the relaxed solid organic-metal interface model is associated with the ionic relaxation energy E_{relax}. The change of energy between the frozen structure of the organic phase obtained from the interface with the metal and the relaxed natural (010) organic surface is the deformation energy E_{def}. The energy difference between the total electronic energy of the relaxed solid organic-metal interface and the references (relaxed clean Pt(111) and natural organic (010) surfaces) is called adhesion energy E_{adh}. The interaction energy $E_{interaction}$ between the frozen organic and metal structures coming from the relaxed interfaces can thus be calculated by subtracting the deformation energy of the organic and the metallic separated systems to the interface energy.

The interface tension is weakly sensitive to the chemical nature of the dissociating molecule (from 1.55 to 1.59 J·m^{-2}). The key reason is the small contribution of the adhesion surface energy γ_{adh} (from -0.03 to 0.01 J·m^{-2}) to the major term γ_{surf}^{met} (1.52 J·m^{-2}).

The deformation energy of the organic surface between the relaxed natural surface (monoclinic phase) and the interface E_{def}^{mol} is dominated by the relaxation term E_{relax}^{mol} for the dissociated state DS and FS of CCl_4/Pt(111), and by the crystalline transition term E_{trans}^{mol} for the molecular state MS of CCl_4/Pt(111) and for ethanol/Pt(111).

The interaction energy between the organic surface and the metal $E_{interac}^{mol/met}$ progressively increases from MS to FS states of CCl_4/Pt(111) (from -91 to -593 kJ·mol^{-1}), in line with the increase of the deformation energy E_{def}^{mol} (from 86 to 420 kJ·mol^{-1}) and in agreement with the dissociation reaction.

The question concerning the consecutive change of the morphology and the density of the organic crystal in contact with platinum can be solved by examining the deformation energy of the organic phase. For both systems, the deformation between the relaxed (010) surface of the organic crystals and the optimized geometry at the interface results in a large energy cost (420 and 266 kJ·mol^{-1} for CCl_4 and ethanol/Pt(111), respectively). For CCl_4/Pt(111), the deformation energy is dominated by the relaxation energy between the optimal geometries of the hexagonal CCl_4(010) surface and of CCl_4 at the interface (340 kJ·mol^{-1}), whereas for ethanol/Pt(111), it is mainly due to the crystalline transition between the monoclinic and the hexagonal ethanol(010) surfaces (140 kJ·mol^{-1}). Hence the crystalline transition imposed by the metal structure and the confinement of the organic surface between the metallic slabs explain the observed dilatation and morphology change occurring after the adhesion of CCl_4 and ethanol films on platinum. This analysis is entirely supported by the electrostatic potential profiles of the organic surfaces (see section 1.6).

1.3 Adsorption strength

The choice of the DFT+D method has been effected by the analysis of the interaction energy $E_{interac}^{mol/met}$ for the adsorption (physisorption) of one ethanol (carbon tetrachloride) molecule on Pt(111) (see gas/Pt systems in Tables 2 and 3) with various levels of calculation and a systematic geometry optimization. For ethanol on Pt(111), the optimal structure is similar to the one obtained at the interface (see Fig. 7) or previously by other authors.[2,3] The adsorption energy (-30.1 kJ·mol^{-1}) at the standard PBE level is already in fair agreement with measurements (from 20 to 54 kJ·mol^{-1} [4,5]). As we can see, the addition of vdW forces only for the atoms of the molecule (-30.8 kJ·mol^{-1} with DFT+D$_{\lambda_2}$) or for all the atoms (-35.2 kJ·mol^{-1} with DFT+D$^*_{\lambda_2}$) does not change really this picture. The interaction energy between the molecule and the metallic surface, ranging from -40.0 to -34.5 kJ·mol^{-1}, dominates all the contributions and the deformation energies are small (below 3 kJ·mol^{-1}). The physisorbed molecular geometry extracted from the solid ethanol/Pt(111) system has also been considered but this has never been found as a local minimum for a single molecule.

For the physisorption of one CCl_4 molecule on Pt(111), the picture is slightly different. Standard PBE already provides a weak physisorbed state (-7 kJ·mol^{-1}) in agreement with the result obtained when vdW forces are included only for the atoms of the molecule (-7.1 kJ·mol^{-1}). The interaction energy is similar in both cases (-7.2 kJ·mol^{-1}) and the deformation energies are absolutely negligible. However, when vdW contributions coming from the metal are considered (DFT+D$^*_{\lambda_1}$ level), the physisorption energy is strongly increased (-31.6 kJ·mol^{-1}). This value is similar to that obtained for the adsorption of ethanol. This questionable result shows undeniably the overestimation of vdW forces between the metal and CCl_4 due to the deficiency of the dispersion coefficients, as evoked previously.[6] For the dissociative adsorption of one CCl_4 molecule (Cl+CCl_{3DS} and Cl+CCl_{3FS}), a large strengthening of the interaction energy is also observed when the metal dispersion energy is included in the calculation (from -278.4 to -313.5 kJ·mol^{-1} and from -481.0 to -533.6 kJ·mol^{-1}, respectively).

Hence a reasonable compromise for the description of energies at the interface is achieved with the DFT+D$_\lambda$ method, where the dispersion contributions are correctly included for the organic phase, and for which the treatment of the weak interactions between the organic phase and the metal is partially satisfactory (at least not overestimated). Moreover the optimized geometries are not strongly modified by the inclusion of the vdW forces coming from the metal (as depicted in Fig. 4 and 7). This justifies our choice of having selected the DFT+D$_\lambda$ method preferentially.

The influence of the organic environment on the adsorption strength is evaluated by comparing the interaction energy between the organic phase and the metal, calculated for the chemisorbed layer at Pt(111) with the one obtained for the organic platinum interface. For ethanol/Pt(111), the interaction energy varies from -105.7 kJ·mol^{-1} for the four chemisorbed molecules in the unit cell to -226.8 kJ·mol^{-1} for the complete film interface at the DFT+D$_{\lambda_2}$ level. The interaction energy between the organic medium and the metal $E_{interac}^{molec/met}$ can be decomposed by separating the contributions coming from the interactions between simpler subgroups of the complete and complex interface model. The interface system can be considered as an assembly of four different subsystems: metal (m), adsorbed layers (a), physisorbed layers (p) and bulk layers (b) (see Fig. 3 for an illustration). At ethanol/Pt(111),

Table 2 Adsorption E_{ads}, physisorption E_{phys}, adhesion E_{adh} energy for various chemical systems at gas, or solid ethanol/Pt(111) interfaces (N_{ads}, N_{phys}, N_{bulk} being the numbers of adsorbed, physisorbed and bulk organic molecules, respectively). The adsorption (adhesion) energy is decomposed into the deformation energy of the molecule (crystal surface) E_{def}^{mol} or the metal E_{def}^{met} and the interaction energy between the molecules and the metal $E_{interac}^{mol/met}$. DFT means standard GGA PBE, DFT+D_{λ_i} means vdW interactions included only for the organic phase and DFT+$D_{\lambda_i}^{*}$ means dispersion energy is considered for all the atoms ($\lambda_2 = 9 \times 10^{-7}$). *sc* means single point energy calculation. The supercell is (4×3) for all systems. All the energies are expressed in kJ·mol^{-1}.

System	Method	Structure	N_{ads}	N_{phys}	N_{bulk}	E_{ads}	E_{phys}	E_{adh}	E_{def}^{mol}	E_{def}^{met}	$E_{interac}^{mol/met}$
gas/Pt											
ethanol	DFT	s_1	1			-30.1			2.7	1.6	-34.5
ethanol	DFT+D_{λ_2}	s_2	1			-30.8			3.0	1.7	-35.5
ethanol	DFT+$D_{\lambda_2}^{*}$	s_3	1			-35.2			3.0	1.7	-40.0
ethanol	DFT	-	2			-58.6					
ethanol	DFT+D_{λ_2}	s_4	2			-62.5			-5.5	4.5	-61.5
ethanol	DFT+$D_{\lambda_2}^{*}$	s_5	2			-71.3					
ethanol	DFT	-	4			-106.2					
ethanol	DFT+D_{λ_2}	s_6	4			-114.8			-11.0	1.9	-105.7
ethanol	DFT+$D_{\lambda_2}^{*}$	s_7	4			-132.3					
(ethanol)	DFT	-	4	4		-214.9					
(ethanol)	DFT+D_{λ_2}	s_8	4	4		-262.2			-69.1	6.5	-199.6
(ethanol)	DFT+$D_{\lambda_2}^{*}$	s_9	4	4		-295.5					
ethanol/Pt											
(ethanol)	DFT+D_{λ_2}	s_{10}	4	4	16			47.3	266.2	7.9	-226.8
(ethanol)	DFT+$D_{\lambda_2}^{*}$	s_{11}	4	4	16			21.9	266.2	7.9	-252.2
ethanol^{sc}	DFT+D_{λ_2}	s_{10}	4	0	0	-71.2			14.5	7.9	-93.7
(ethanol)^{sc}	DFT+D_{λ_2}	s_{10}	0	4	0		-41.8		-10.6	7.9	-39.1
(ethanol)^{sc}	DFT+D_{λ_2}	s_{10}	4	4	0	-237.4			-59.2	7.9	-186.2
(ethanol)^{sc}	DFT+D_{λ_2}	s_{10}	0	0	16		-656.8		-659.9	7.9	-4.9
(ethanol)^{sc}	DFT+D_{λ_2}	s_{10}	4	0	16	-771.0			-695.2	7.9	-83.7
(ethanol)^{sc}	DFT+D_{λ_2}	s_{10}	0	4	16		-745.7		-717.2	7.9	-36.4

Table 3 Adsorption E_{ads}, physisorption E_{phys}, adhesion E_{adh} energy for various chemical systems at gas, or CCl_4/Pt(111) interfaces (N_{ads}, N_{phys}, N_{bulk} being the numbers of adsorbed, physisorbed and bulk organic molecules, respectively). The adsorption (adhesion) energy is decomposed into the deformation energy of the molecule (crystal surface) E_{def}^{mol} or the metal E_{def}^{met} and the interaction energy between the molecules and the metal $E_{interac}^{mol/met}$. DFT means standard GGA PBE. At DFT+D_{λ_i} level, vdW interactions are included only for the organic phase while at DFT+$D^*_{\lambda_i}$ level, dispersion energy is considered for all the atoms ($\lambda_1 = 10^{-3}$). *sc* means single point energy calculation. The supercell is (7×7) for all systems. All the energies are expressed in kJ·mol^{-1}.

System	Method	Structure	N_{ads}	N_{phys}	N_{bulk}	E_{ads}	E_{phys}	E_{adh}	E_{def}^{mol}	E_{def}^{met}	$E_{interac}^{mol/met}$
gas/Pt											
$CCl_{4_{MS}}$	DFT	s_1		1			-7.0		0.05	0.1	-7.2
$CCl_{4_{MS}}$	DFT+D_{λ_1}	s_2		1			-7.1		0.03	0.08	-7.2
$CCl_{4_{MS}}$	DFT+$D^*_{\lambda_1}$	s_3		1			-31.6		0.03	0.06	-31.7
$Cl+CCl_{3_{DS}}$	DFT	s_4	1			6.5			279.6	5.2	-278.4
$Cl+CCl_{3_{DS}}$	DFT+D_{λ_1}	s_5	1			5.2			278.8	4.8	-278.4
$Cl+CCl_{3_{DS}}$	DFT+$D^*_{\lambda_1}$	s_6	1			-29.8			279.0	4.7	-313.5
$Cl+CCl_{3_{FS}}$	DFT	s_7	1			-115.4			333.9	31.7	-481.0
$Cl+CCl_{3_{FS}}$	DFT+D_{λ_1}	s_8	1			-115.8			333.5	31.7	-481.0
$Cl+CCl_{3_{FS}}$	DFT+$D^*_{\lambda_1}$	s_9	1			-163.7			339.2	30.7	-533.6
$(CCl_4)_{DS}$	DFT	-		15			-123.9				
$(CCl_4)_{DS}$	DFT+D_{λ_1}	s_{10}		15			-175.5		-129.4	0.8	-46.9
$(CCl_4)_{DS}$	DFT+$D^*_{\lambda_1}$	s_{11}		15			-581.7				
$(Cl+CCl_3)_{DS}$	DFT	-	1	15		-118.5					
$(Cl+CCl_3)_{DS}$	DFT+D_{λ_1}	s_{12}	1	15		-199.4			26.2	5.5	-231.1
$(Cl+CCl_3)_{DS}$	DFT+$D^*_{\lambda_1}$	s_{13}	1	15		-636.5					
CCl_4/Pt											
$(CCl_4)_{MS}$	DFT+D_{λ_1}	s_{14}	0	16	24			-3.8	86.3	0.5	-90.6
$(CCl_4)_{MS}$	DFT+$D^*_{\lambda_1}$	s_{15}	0	16	24			-480.7	86.3	0.4	-567.4
$(Cl+CCl_3)_{DS}$	DFT+D_{λ_1}	s_{16}	1	15	24			11.2	250.5	5.8	-245.1
$(Cl+CCl_3)_{DS}$	DFT+$D^*_{\lambda_1}$	s_{17}	1	15	24			-478.7	250.5	5.9	-735.1
$(Cl+CCl_3)_{FS}$	DFT+D_{λ_1}	s_{18}	1	15	24			-138.8	420.3	33.6	-592.7
$(Cl+CCl_3)_{FS}$	DFT+$D^*_{\lambda_1}$	s_{19}	1	15	24			-702.8	398.4	33.2	-1134.4
Cl^{sc}_{DS}	DFT+D_{λ_1}	s_{16}	1	0	0	-240.3			0.0	5.9	-246.2
$(Cl)^{sc}_{DS}$	DFT+D_{λ_1}	s_{16}	1	15	0	-404.7			-105.6	5.9	-305.1
$(Cl)^{sc}_{DS}$	DFT+D_{λ_1}	s_{16}	1	0	24	-655.6			-366.2	5.9	-295.3
$(Cl)^{sc}_{DS}$	DFT+D_{λ_1}	s_{16}	1	15	24	-1039.1			-705.3	5.9	-339.7
$CCl_3{}^{sc}_{DS}$	DFT+D_{λ_1}	s_{16}	1	0	0	-21.8			7.2	5.9	-34.9
$(CCl_3)^{sc}_{DS}$	DFT+D_{λ_1}	s_{16}	1	15	0	-196.4			-133.7	5.9	-68.6
$(CCl_3)^{sc}_{DS}$	DFT+D_{λ_1}	s_{16}	1	0	24	-443.2			-447.1	5.9	-2.0
$(CCl_3)^{sc}_{DS}$	DFT+D_{λ_1}	s_{16}	1	15	24	-834.9			-820.1	5.9	-20.7
$Cl+CCl_3{}^{sc}_{DS}$	DFT+D_{λ_1}	s_{16}	1	0	0	5.9			280.1	5.9	-280.1
$(Cl+CCl_3)^{sc}_{DS}$	DFT+D_{λ_1}	s_{16}	1	15	0	-171.0			36.7	5.9	-213.7
$(Cl+CCl_3)^{sc}_{DS}$	DFT+D_{λ_1}	s_{16}	1	0	24	-416.2			-201.1	5.9	-221.0
$(CCl_4)^{sc}_{DS}$	DFT+D_{λ_1}	s_{16}	0	15	0		-175.0		-129.4	5.9	-51.5
$(CCl_4)^{sc}_{DS}$	DFT+D_{λ_1}	s_{16}	0	0	24		-408.3		-370.9	5.9	-43.3
$(CCl_4)^{sc}_{DS}$	DFT+D_{λ_1}	s_{16}	0	15	24		-788.7		-707.8	5.9	-86.8
Cl^{sc}_{FS}	DFT+D_{λ_1}	s_{18}	1	0	0	-243.4			0.0	33.6	-277.0
$(Cl)^{sc}_{FS}$	DFT+D_{λ_1}	s_{18}	1	15	0	-426.4			-108.6	33.6	-351.3
$(Cl)^{sc}_{FS}$	DFT+D_{λ_1}	s_{18}	1	0	24	-670.9			-375.5	33.6	-328.9
$(Cl)^{sc}_{FS}$	DFT+D_{λ_1}	s_{18}	1	15	24	-1078.9			-727.2	33.6	-385.3
$CCl_3{}^{sc}_{FS}$	DFT+D_{λ_1}	s_{18}	1	0	0	-119.1			65.2	33.6	-217.9
$(CCl_3)^{sc}_{FS}$	DFT+D_{λ_1}	s_{18}	1	15	0	-306.8			-74.6	33.6	-265.7
$(CCl_3)^{sc}_{FS}$	DFT+D_{λ_1}	s_{18}	1	0	24	-548.8			-324.3	33.6	-258.0
$(CCl_3)^{sc}_{FS}$	DFT+D_{λ_1}	s_{18}	1	15	24	-961.3			-697.3	33.6	-297.6
$Cl+CCl_3{}^{sc}_{FS}$	DFT+D_{λ_1}	s_{18}	1	0	0	-115.4			342.9	33.6	-491.8
$(Cl+CCl_3)^{sc}_{FS}$	DFT+D_{λ_1}	s_{18}	1	15	0	-304.9			224.7	33.6	-563.2
$(Cl+CCl_3)^{sc}_{FS}$	DFT+D_{λ_1}	s_{18}	1	0	24	-545.9			-45.5	33.6	-534.0
$(CCl_4)^{sc}_{FS}$	DFT+D_{λ_1}	s_{18}	0	15	0		-147.2		-124.8	33.6	-56.0
$(CCl_4)^{sc}_{FS}$	DFT+D_{λ_1}	s_{18}	0	0	24		-392.9		-390.5	33.6	-36.0
$(CCl_4)^{sc}_{FS}$	DFT+D_{λ_1}	s_{18}	0	15	24		-798.9		-745.0	33.6	-87.5

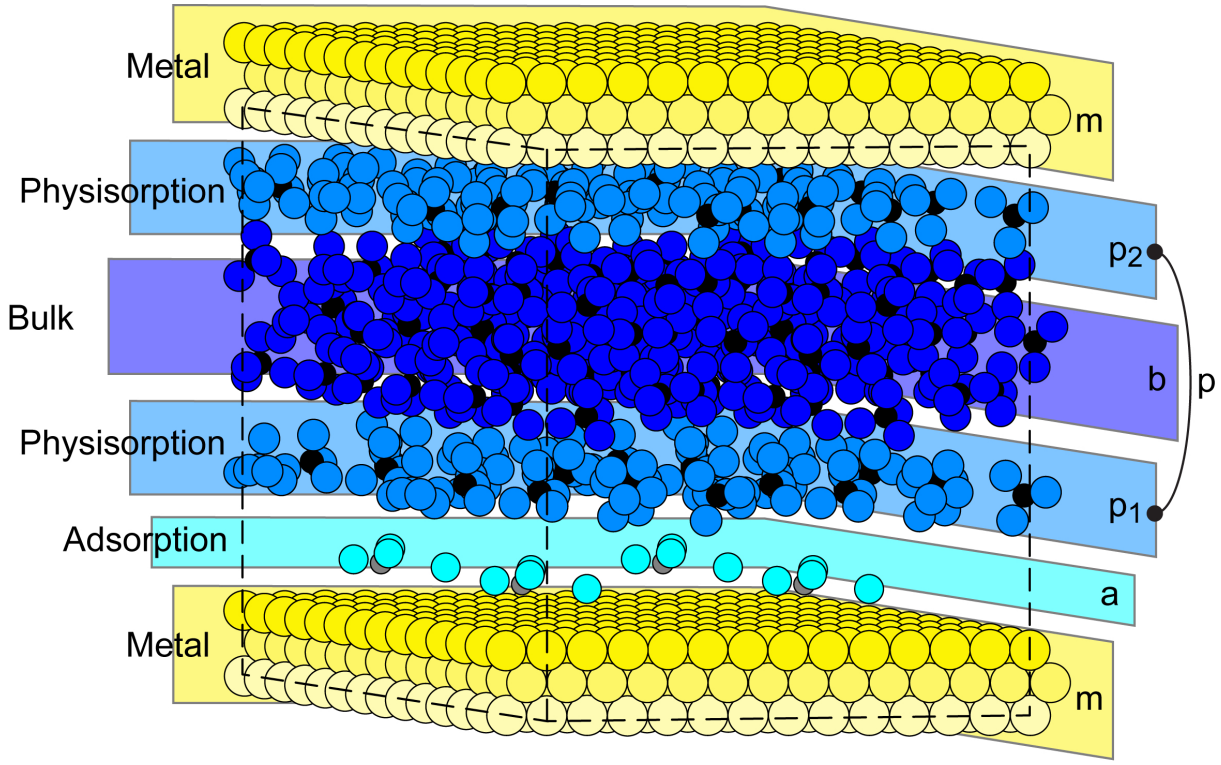

Fig. 3 Scheme illustrating the decomposition of the interface model in an assembly of four simpler subsystems.

the effective interaction energy between the chemisorbed ethanol molecules and the metal (-190.5 kJ·mol^{-1}) is thus derived from the difference between the complete interface system (-226.8 kJ·mol^{-1}) and the contributions arising from the surrounding physisorbed and the bulk molecules (-36.4 kJ·mol^{-1}). So the actual gain is -96.8 kJ·mol^{-1} by comparison with the interaction energy of the four chemisorbed molecules at Pt(111) (-93.7 kJ·mol^{-1}). The normalized gain is thus -24.2 kJ·mol^{-1} per ethanol chemisorbed molecule. The normalized loss due to metal-adsorbate relaxation is very weak (+3 kJ·mol^{-1}).

For CCl_4/Pt(111), a similar analysis can be drawn. The interaction energy between the adsorbed dissociated species Cl+CCl_3 in the most stable structure (FS) and platinum changes from -481 kJ·mol^{-1} (optimal single adsorption or -491.8 kJ·mol^{-1} at the interface) to -592.7 kJ·mol^{-1} (complete interface system). The effective interaction energy between the adsorbate and the metal is -505.2 kJ·mol^{-1} (in the absence of the surrounding molecules). The adsorption strength is thus increased to a lesser extent with a gain of -13.3 kJ·mol^{-1} per Cl+CCl_3 chemisorbed species.

1.4 Interaction energy decomposition model

Generally, when two subsystems (A and B) are interacting in the same time with a third one (C), the corresponding three-body interaction energy $E^{int}_{(A+B)-C}$ can be linearized in a sum of three two-body contributions as follows:

$$E^{int}_{(A+B)-C} = E^{int}_{A-C} + E^{int}_{B-C} + \tilde{E}^{int}_{A-B} \qquad (12)$$

If the two-body terms E^{int}_{A-C} and E^{int}_{B-C} are calculated separately with the three-body term $E^{int}_{(A+B)-C}$, the non-additive term $\tilde{E}^{int}_{A-B}$ corresponding to the interaction energy between (A) and (B) in presence of (C) is thus simply evaluated by subtracting the three other contributions. In our case, (C) is the metal while (A) and (B) can be alternatively the adsorbed, physisorbed and bulk organic layers.

In Tables 2 and 3, the interaction energies of the subsystems forming the interfaces of solid ethanol/Pt(111) and CCl_4/Pt(111) are summarized. Most of the subsystems corresponding to adsorption, physisorption alone or both of them, have been reoptimized. Each optimized structure is noted s_i and the corresponding geometries are depicted in Fig. 4, 5, 6, 7 and 8. Different levels of calculation have been tested in order to evaluate the van der Waals contributions resulting from the organic phase and the metallic partner. The DFT+D

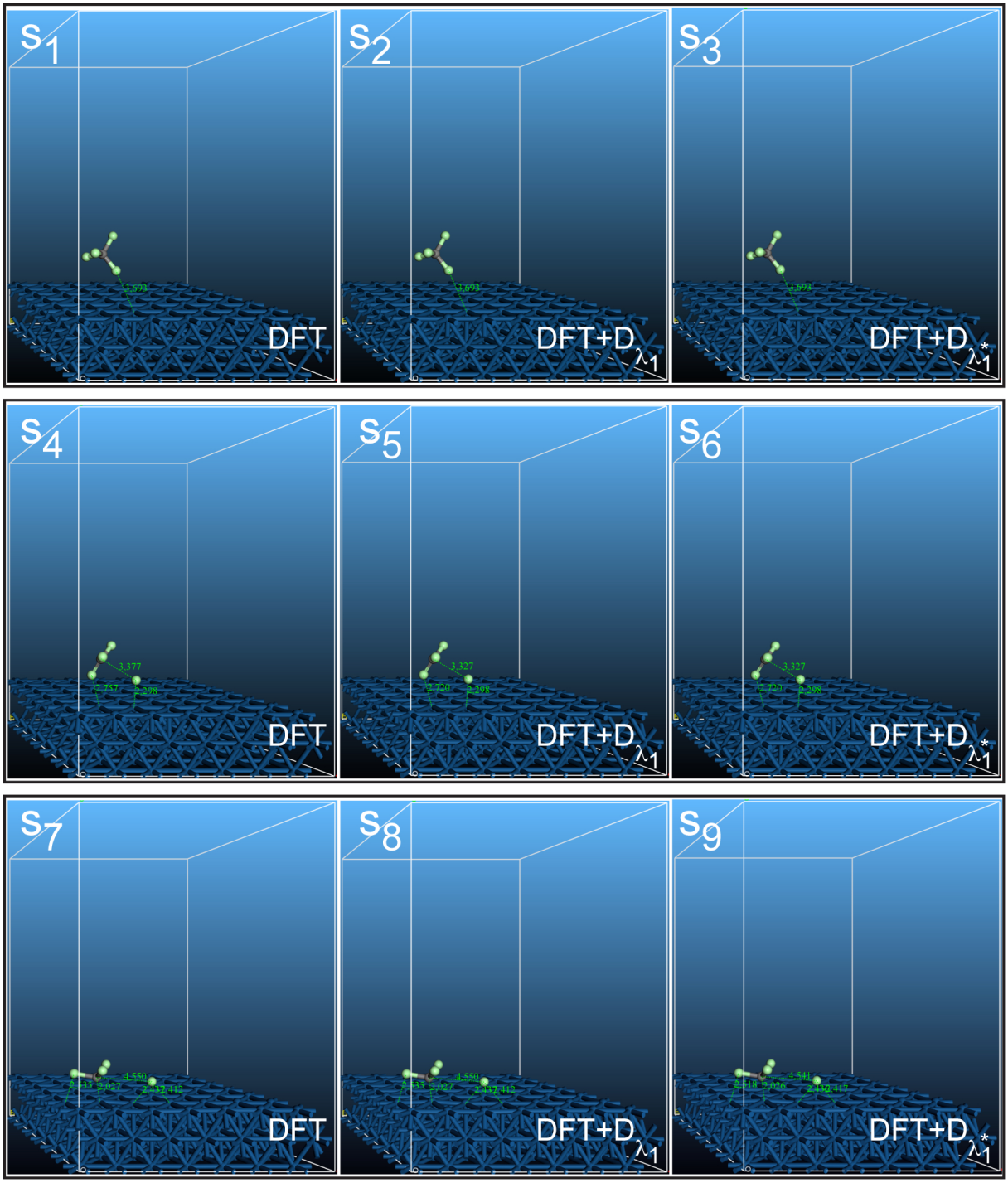

Fig. 4 Optimized structures for decomposing the adsorption strength at solid CCl_4/Pt(111) interface. Some key distances are given in Å.

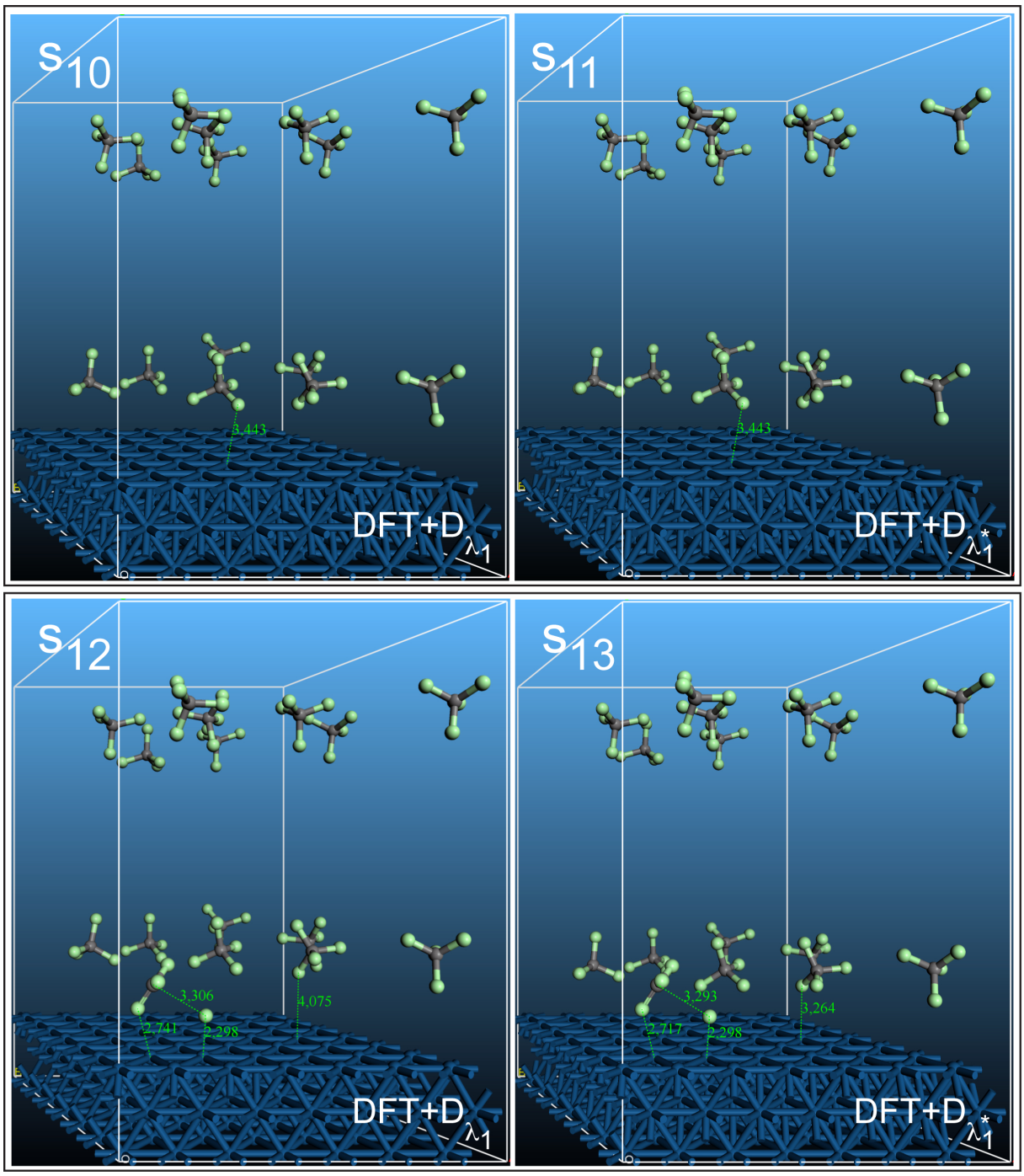

Fig. 5 Optimized structures for decomposing the adsorption strength at solid CCl_4/Pt(111) interface. Some key distances are given in Å.

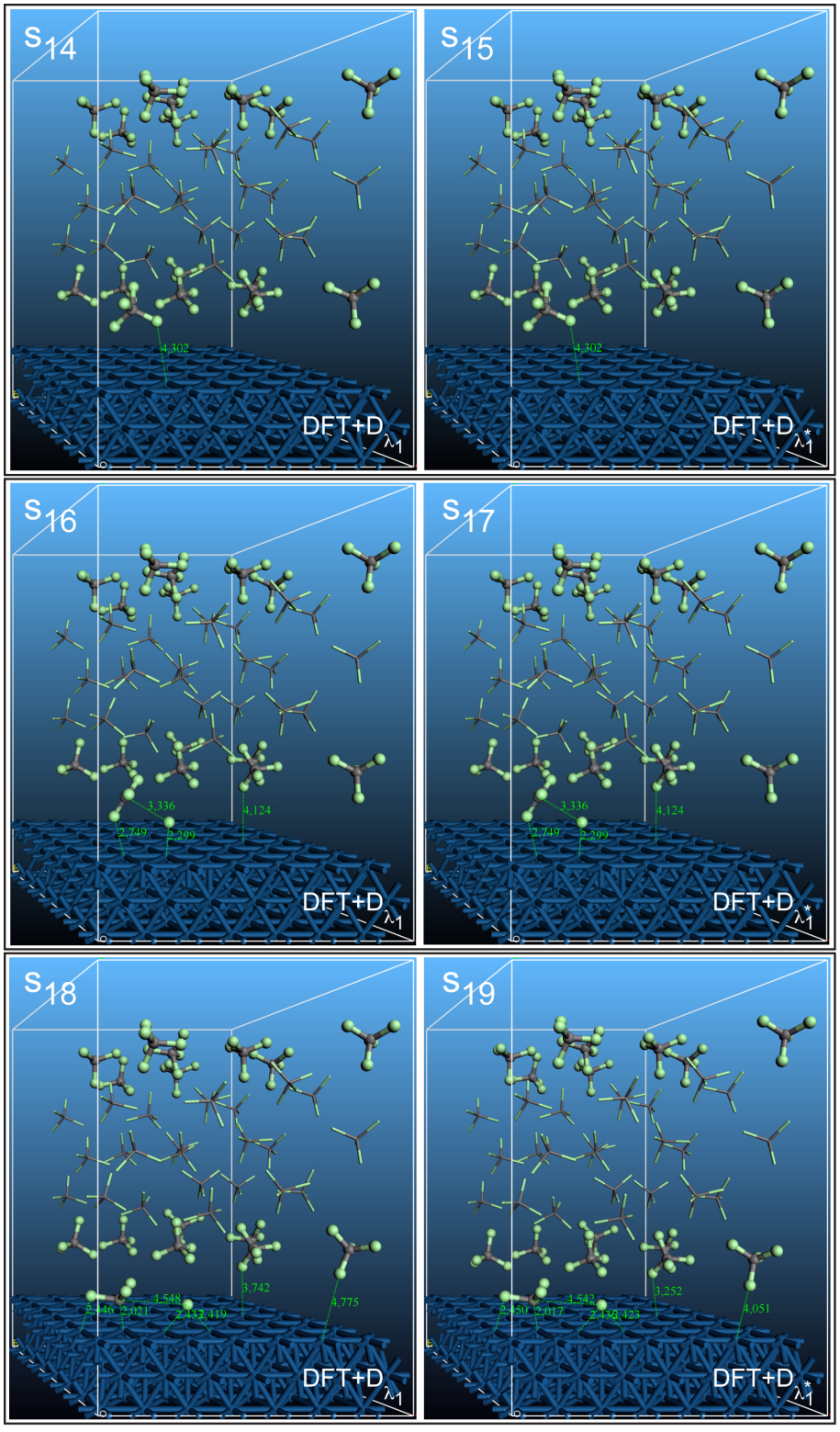

Fig. 6 Optimized structures for decomposing the adsorption strength at solid CCl_4/Pt(111) interface. Some key distances are given in Å.

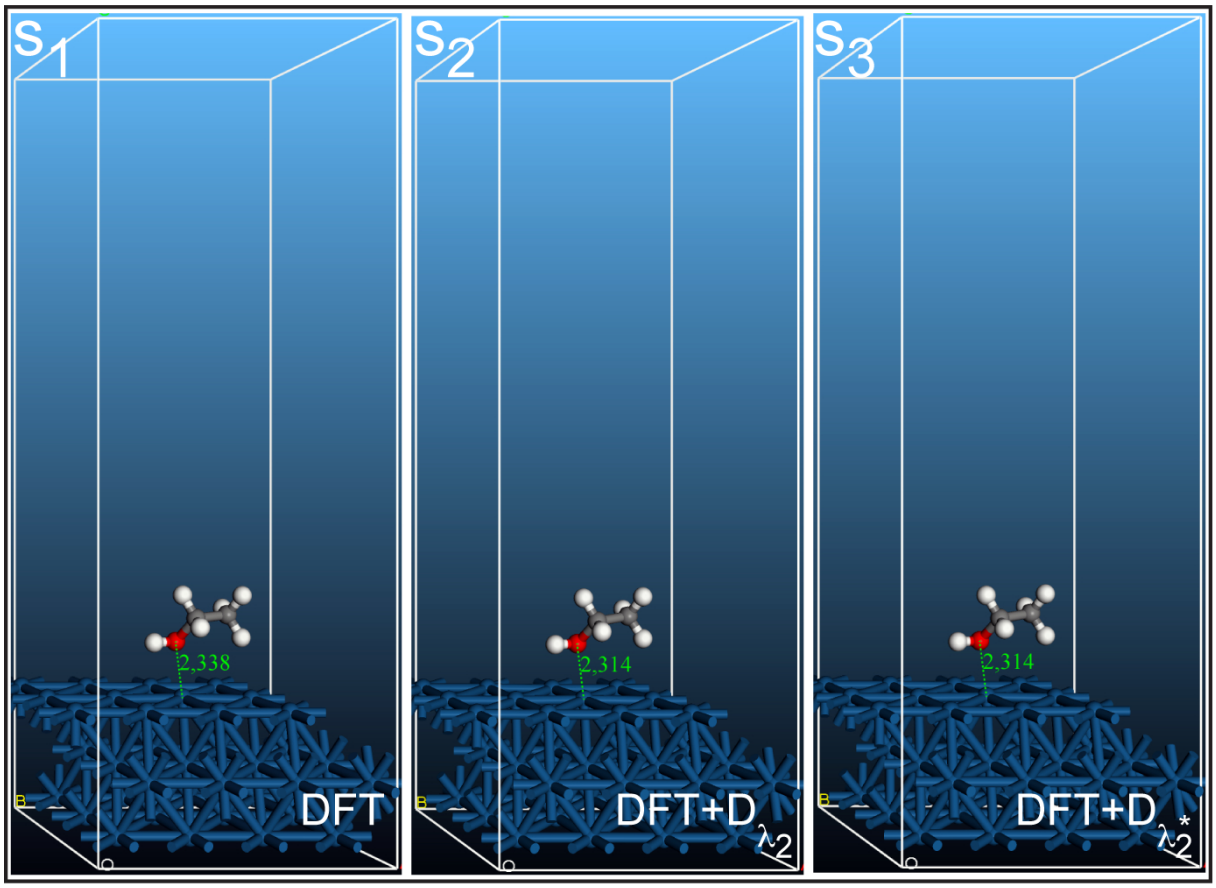

Fig. 7 Optimized structures for decomposing the adsorption strength at solid ethanol/Pt(111) interface. Some key distances are given in Å.

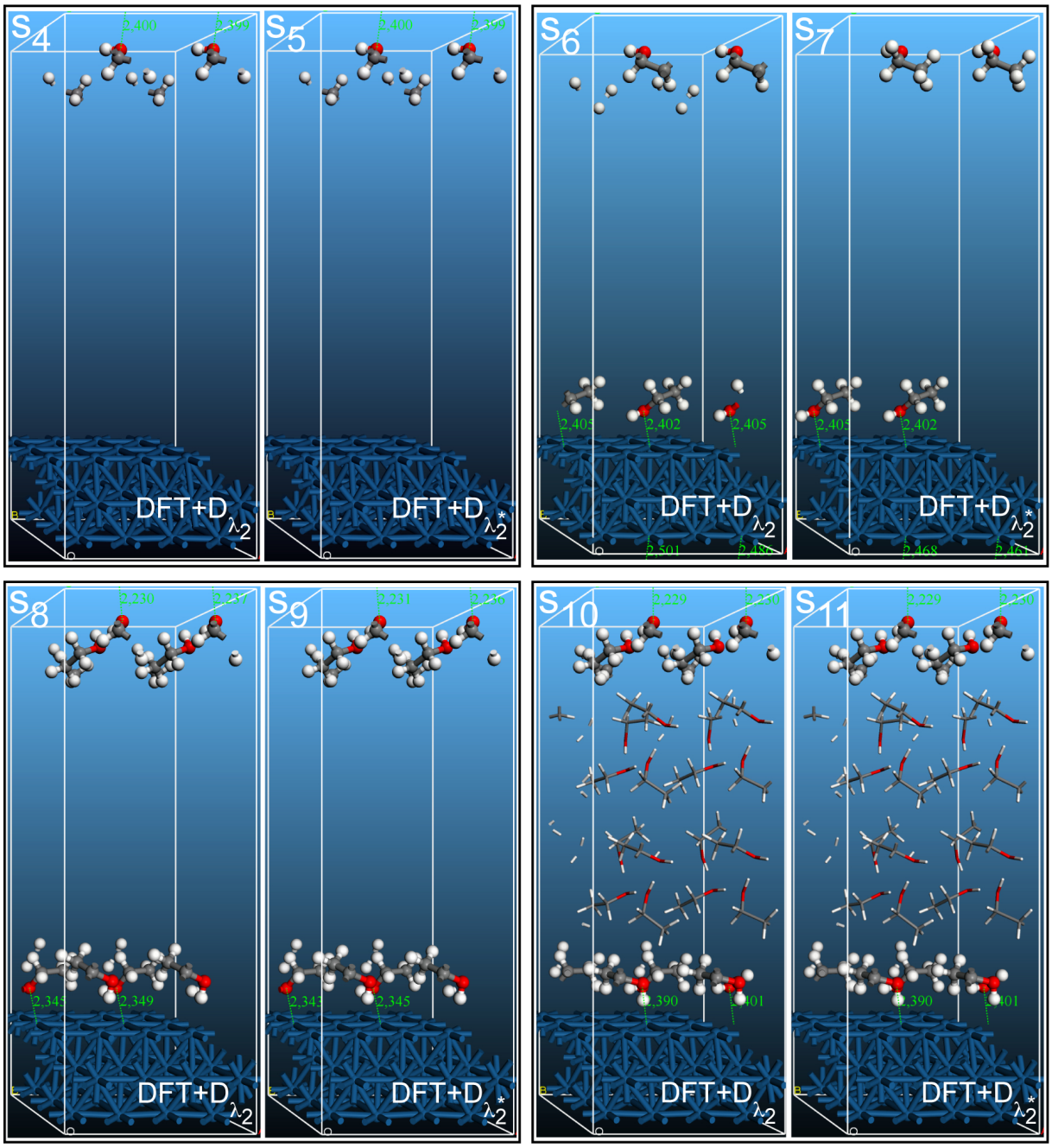

Fig. 8 Optimized structures for decomposing the adsorption strength at solid ethanol/Pt(111) interface. Some key distances are given in Å.

Table 4 Decomposition model of the interaction energy between the adsorbed layers (a) and the metal (m) by considering the contributions resulting from the physisorbed (p) and the bulk layers (b). For ethanol/Pt(111), the used structure of the interface s_{10} is the optimal one reported in Fig. 8. The values written in parentheses are the normalized interaction energies since the adsorbed layer is composed of four ethanol molecules. For CCl_4/Pt(111), the results of the two dissociated states (DS) and (FS) (structures s_{16} and s_{18} in Fig. 6, respectively) are indicated. All the energies are expressed in kJ·mol^{-1}. An illustration of some of these energetic terms is available in Fig. 9.

Structure	ethanol/Pt(111) s_{10}	CCl_4/Pt(111) s_{16} (DS)	CCl_4/Pt(111) s_{18} (FS)
$E^{int}_{(a+p+b)-m}$	-226.8	-245.1	-592.7
E^{int}_{a-m}	-93.7 (-23.4)	-280.1	-491.8
$E^{int}_{(p+b)-m}$	-36.4	-87.1	-87.5
$\tilde{E}^{int}_{a-(p+b)}$	-96.8 (-24.2)	122.1	-13.3
$E^{int,eff}_{a-m}$	-190.5 (-47.6)	-158.0	-505.2
$E^{int}_{(a+p)-m}$	-186.2	-213.7	-563.2
E^{int}_{p-m}	-39.1 (-9.8)	-51.5	-56.0
$E^{int}_{(a+b)-m}$	-83.7	-221.0	-534.0
E^{int}_{b-m}	-4.9 (-0.3)	-43.3	-36.0
$\tilde{E}^{int}_{a-p}$	-53.4 (-13.3)	118.0	-15.4
$\tilde{E}^{int}_{a-b}$	14.8 (3.7)	102.4	-6.2
$\tilde{E}^{int}_{p-b}$	7.6	7.7	4.4
$\tilde{E}^{(a),int}_{p-b}$	-50.7	-90.6	12.6
$\Delta\tilde{E}^{(\oslash\rightarrow a),int}_{p-b}$	-58.3 (-14.6)	-98.3	8.2
$E^{int}_{(a3+p+b)-m}$	*	-20.7	-297.6
E^{int}_{a3-m}	*	-34.9	-217.9
$\tilde{E}^{int}_{a3-(p+b)}$	*	101.3	7.9
$E^{int,eff}_{a3-m}$	*	66.4	-210.0
$E^{int}_{(a1+p+b)-m}$	*	-339.7	-385.3
E^{int}_{a1-m}	*	-246.2	-277.0
$\tilde{E}^{int}_{a1-(p+b)}$	*	-6.4	-20.8
$E^{int,eff}_{a1-m}$	*	-252.6	-297.8
$E^{int}_{(a3+p)-m}$	*	-68.6	-265.7
$E^{int}_{(a3+b)-m}$	*	-2.0	-258.0
$E^{int}_{(a1+p)-m}$	*	-305.1	-351.3
$E^{int}_{(a1+b)-m}$	*	-295.3	-328.9
$\tilde{E}^{int}_{a3-p}$	*	17.8	8.2
$\tilde{E}^{int}_{a3-b}$	*	76.1	-4.1
$\tilde{E}^{(a3),int}_{p-b}$	*	15.1	8.2
$\Delta\tilde{E}^{(\oslash\rightarrow a3),int}_{p-b}$	*	7.3	3.8
$\tilde{E}^{int}_{a1-p}$	*	-7.3	-18.3
$\tilde{E}^{int}_{a1-b}$	*	-5.8	-15.9
$\tilde{E}^{(a1),int}_{p-b}$	*	14.5	17.9
$\Delta\tilde{E}^{(\oslash\rightarrow a1),int}_{p-b}$	*	6.7	13.5
$\tilde{E}^{(\oslash),int}_{a3-a1}$	*	1.0	3.1
$\tilde{E}^{(p),int}_{a3-a1}$	*	160.0	53.8
$\tilde{E}^{(b),int}_{a3-a1}$	*	76.4	53.0
$\tilde{E}^{(p+b),int}_{a3-a1}$	*	115.3	90.2

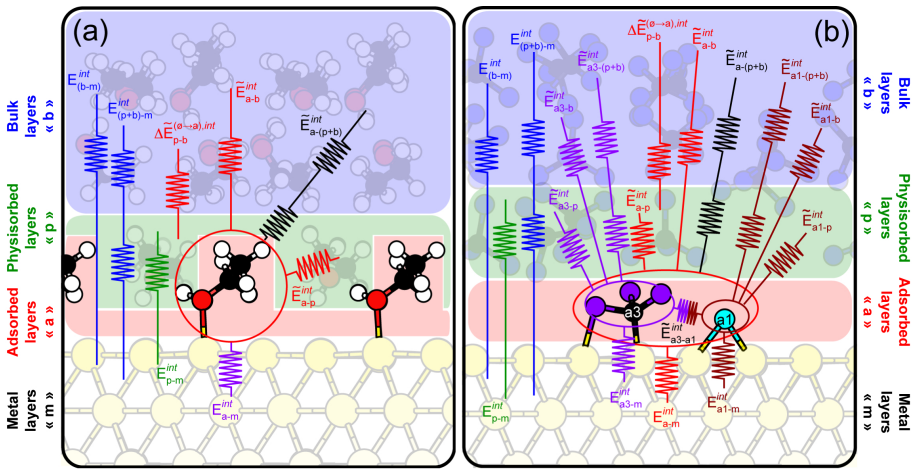

Fig. 9 Scheme illustrating some of the interaction energies of the subsystems composing the interface models (a) ethanol/Pt(111) and (b) CCl_4/Pt(111) (FS). The corresponding values are listed in Table 4.

notations are equivalent to those of the manuscript. Moreover, the results of the optimal interface systems have been also reported and completed with different DFT+D levels of calculation.

Coming back to the decomposition of the interaction energy between the organic phase (a+p+b) and the metal (m) $E^{int}_{(a+p+b)-m}$, we have applied the linearization principle of Eq. (12) to the complete interface system (a+p+b+m) and to the subsystems (a+p+m), (a+b+m) and (p+b+m):

$$E^{int}_{(a+p+b)-m} = E^{int}_{a-m} + E^{int}_{(p+b)-m} + \tilde{E}^{int}_{a-(p+b)} \quad (13)$$

$$E^{int}_{(a+p)-m} = E^{int}_{a-m} + E^{int}_{p-m} + \tilde{E}^{int}_{a-p} \quad (14)$$

$$E^{int}_{(a+b)-m} = E^{int}_{a-m} + E^{int}_{b-m} + \tilde{E}^{int}_{a-b} \quad (15)$$

$$E^{int}_{(p+b)-m} = E^{int}_{p-m} + E^{int}_{b-m} + \tilde{E}^{int}_{p-b} \quad (16)$$

In order to calculate all the corresponding interaction terms, the subsystems forming the complete interface models have also been considered by freezing their geometries in the ones obtained in the interfaces. All the corresponding results have also been presented in Tables 2 and 3 with the specific notation *sc* for single-point energy calculation (meaning without reoptimization).

The next step is the determination of the interaction energy between the adsorbate and the other physisorbed and bulk layers $\tilde{E}^{int}_{a-(p+b)}$, in order to evaluate the perturbation of the organic medium on the adsorption strength between the adsorbed layer and the metal. By combining Eq. (14)+(15)-(16) and then using Eq. (13), one can derive the complex following equation:

$$\tilde{E}^{int}_{a-(p+b)} = (E^{int}_{(a+p+b)-m} + E^{int}_{a-m}) - (E^{int}_{(a+p)-m} + E^{int}_{(a+b)-m}) + \tilde{E}^{int}_{a-p} + \tilde{E}^{int}_{a-b} - \tilde{E}^{int}_{p-b} \quad (17)$$

In Eq. (17), the first two terms correspond to the interaction energy between the physisorbed and the bulk organic layers in the presence of the adsorbate, by opposition with the previously defined interaction energy $\tilde{E}^{int}_{p-b}$ calculated without the adsorbed layers. By noting this new term $\tilde{E}^{(a),int}_{p-b}$ and by defining the variation of this interaction energy $\Delta\tilde{E}^{(\oslash\rightarrow a),int}_{p-b}$, we derive the following expressions:

$$\tilde{E}^{(a),int}_{p-b} = (E^{int}_{(a+p+b)-m} + E^{int}_{a-m}) - (E^{int}_{(a+p)-m} + E^{int}_{(a+b)-m}) \quad (18)$$

$$\Delta\tilde{E}^{(\oslash\rightarrow a),int}_{p-b} = \tilde{E}^{(a),int}_{p-b} - \tilde{E}^{int}_{p-b} \quad (19)$$

$$\tilde{E}^{int}_{a-(p+b)} = \tilde{E}^{int}_{a-p} + \tilde{E}^{int}_{a-b} + \Delta\tilde{E}^{(\oslash\rightarrow a),int}_{p-b} \quad (20)$$

Hence in our model, the perturbation on the adsorbed layers due to the organic medium above $\tilde{E}^{int}_{a-(p+b)}$ has been decomposed in a sum of three simpler interaction terms, as shown in Eq. (20). The effective interaction energy between the adsorbate and the metal in the presence of the organic phase $E^{int,eff}_{a-m}$ is then defined by substracting the interaction energy between the physisorbed and bulk layers and the metal $E^{int}_{(p+b)-m}$ to the initial term $E^{int}_{(a+p+b)-m}$. By using, once again Eq. (13), one can easily derive the following equations linking $\tilde{E}^{int}_{a-(p+b)}$ with the variation of the adsorption strength between the adsorbate and the metal ΔE^{int}_{a-m}:

$$E^{int,eff}_{a-m} = E^{int}_{(a+p+b)-m} - E^{int}_{(p+b)-m} = E^{int}_{a-m} + \tilde{E}^{int}_{a-(p+b)} \quad (21)$$

$$\tilde{E}^{int}_{a-(p+b)} = E^{int,eff}_{a-m} - E^{int}_{a-m} = \Delta E^{int}_{a-m} \quad (22)$$

In conclusion, one can evaluate the perturbation on the adsorption strength due to the organic phase just by evaluating $\tilde{E}^{int}_{a-(p+b)}$. Moreover, such a perturbation is finally decomposed in three explicit contributions:

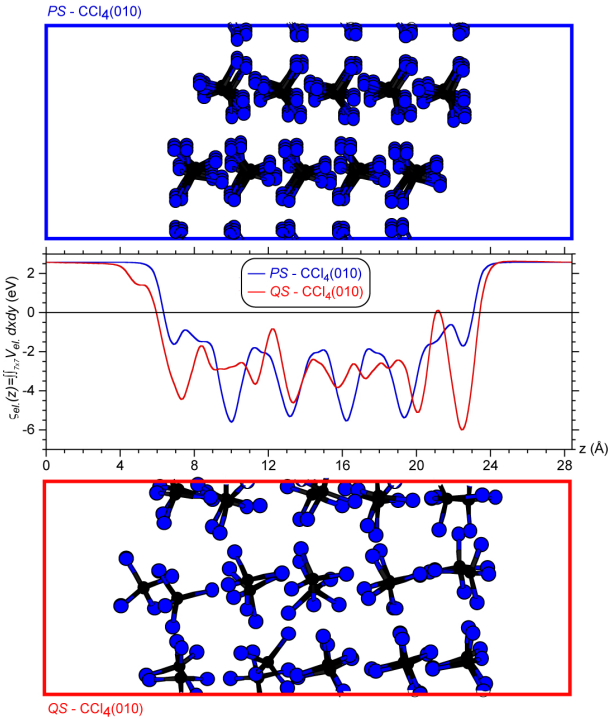

Fig. 10 Average electrostatic potential $\zeta(z)$ (eV) along z axis (Å) for solid $CCl_4(010)$ surfaces with (a) monoclinic phase (PS, blue curve) and (b) hexagonal phase (QS, red curve).

- a direct contribution due to the interaction energy between the adsorbed and the physisorbed layers $\tilde{E}^{int}_{a-p}$
- a direct contribution due to the interaction energy between the adsorbed and the bulk layers $\tilde{E}^{int}_{a-b}$
- an indirect contribution due to the variation of the interaction energy between the physisorbed and the bulk layers, as a retroactive response of the solvent due to presence of the adsorbate $\Delta\tilde{E}^{(\oslash\rightarrow a),int}_{p-b}$

In Table 4, the results of this decomposition are exposed for CCl_4/Pt(111) and ethanol/Pt(111) interfaces using the elementary interaction energies previously given in Tables 2 and 3. For CCl_4/Pt(111), the results of the two dissociated states DS and FS are presented. Furthermore, for these latter interface systems, the adsorbed layers have an intrinsic additional complexity due to the coadsorption between CCl_3 and Cl. We have thus applied the decomposition model by considering each of adsorbates separately. The notations are (a3) for CCl_3 adsorbed species and (a1) for Cl. An illustration of the definitions of all these interaction energies is also given in Fig. 9 in order to guide the reader.

The last difficulty is the determination of the interaction energy between CCl_3 and Cl adsorbates in the presence of the metal (or contact energy). The picture is rather complex since this energetic term can be calculated only with the metal $\tilde{E}^{(\oslash),int}_{a3-a1}$, or alternatively with the additional presence of the physisorbed layers $\tilde{E}^{(p),int}_{a3-a1}$, or the bulk layers $\tilde{E}^{(b),int}_{a3-a1}$, or both of them $\tilde{E}^{(p+b),int}_{a3-a1}$. All the corresponding equations are listed hereafter and the results are given in Table 4:

$$\tilde{E}^{(\oslash),int}_{a3-a1} = E^{int}_{(a3+a1)-m} - (E^{int}_{a3-m} + E^{int}_{a1-m}) \quad (23)$$

$$\tilde{E}^{(p),int}_{a3-a1} = E^{int}_{(a3+a1)-(m+p)} - (E^{int}_{a3-(m+p)} + E^{int}_{a1-(m+p)}) \quad (24)$$

$$\tilde{E}^{(b),int}_{a3-a1} = E^{int}_{(a3+a1)-(m+b)} - (E^{int}_{a3-(m+b)} + E^{int}_{a1-(m+b)}) \quad (25)$$

$$\tilde{E}^{(p+b),int}_{a3-a1} = E^{int}_{(a3+a1)-(m+p+b)} - (E^{int}_{a3-(m+p+b)} + E^{int}_{a1-(m+p+b)}) \quad (26)$$

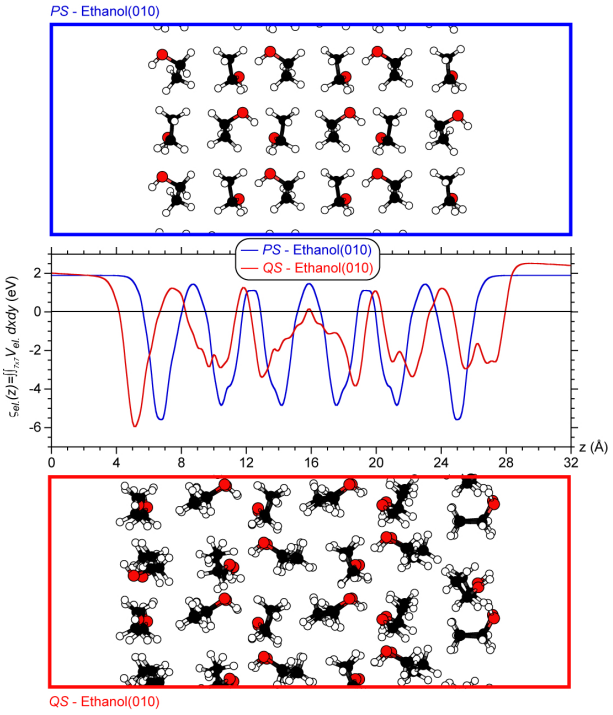

Fig. 11 Average electrostatic potential $\zeta(z)$ (eV) along z axis (Å) for solid ethanol(010) surfaces with (a) monoclinic phase (PS, blue curve) and (b) hexagonal phase (QS, red curve).

1.5 Workfunction and surface dipole changes

The workfunction Φ of any system is defined as follows:

$$\Phi = W_s - E_F \quad (27)$$

Table 5 Fermi level energy E_F, vacuum potential or potential energy difference across the surface due to effective surface dipole W_s, workfunction Φ and variations of workfunction $\Delta\Phi$, surface dipole ΔW_s and Fermi energy ΔE_F for solid CCl_4/Pt(111) and ethanol/Pt(111) interfaces and adsorbed Cl+CCl_3 and four coadsorbed ethanol molecules on Pt(111) with respect to clean Pt surfaces. All the energies are given in eV.

	Supercell	E_F	W_s	Φ	$\Delta\Phi^{clean\to i}$	$\Delta W_s^{clean\to i}$	$\Delta E_F^{clean\to i}$
$(CCl_4)_{DS}$/Pt(111)	(7×7)	-1.30	4.35	5.66	-0.10	1.26	1.35
$(CCl_4)_{FS}$/Pt(111)	(7×7)	-1.38	4.33	5.71	-0.04	1.24	1.28
$(CCl_4)_{DS}$	(7×7)	-2.06	3.56	5.63			
$(CCl_4)_{FS}$	(7×7)	-3.85	2.81	6.66			
CCl_{4MS}/Pt(111)	(7×7)	-2.56	3.18	5.74	-0.01	0.08	0.10
Cl+CCl_{3DS}/Pt(111)	(7×7)	-2.43	3.18	5.62	-0.14	0.08	0.22
Cl+CCl_{3FS}/Pt(111)	(7×7)	-2.54	3.18	5.72	-0.03	0.08	0.11
Clean Pt(111)	(7×7)	-2.66	3.10	5.75			
	Supercell	E_F	W_s	Φ	$\Delta\Phi^{clean\to i}$	$\Delta W_s^{clean\to i}$	$\Delta E_F^{clean\to i}$
(ethanol)/Pt(111)	(4×3)	-1.52	4.06	5.58	-0.20	1.30	1.49
(ethanol)	(4×3)	-2.78	2.85	5.63			
1 ethanol/Pt(111)	(4×3)	-2.47	2.79	5.25	-0.52	0.02	0.54
4 ethanol/Pt(111)	(4×3)	-1.44	2.77	4.21	-1.57	0.00	1.57
Clean Pt(111)	(4×3)	-3.00	2.77	5.78			

where W_s is the vacuum potential or the potential energy difference across the surface due to effective surface dipole and E_F is the Fermi level energy. The corresponding calculated energies are reported in Table 5. The variations of the workfunction from the clean Pt(111) surface to the single adsorption $\Delta\Phi^{clean\to i}$ shows a larger change for coadsorbed ethanol (-1.57 eV) than for the adsorbed species Cl+CCl_3 in the (FS) structure (-0.03 eV). In both cases, this variation is entirely due to the change of the calculated Fermi level. When the molecule is then immersed at the interface, the change of $\Delta\Phi^{clean\to i}$ is again much larger for ethanol/Pt(111) (-0.20 eV) than for CCl_4/Pt(111) (-0.04 eV) for (FS). In both cases, the values of $\Delta\Delta\Phi^{clean\to i}$ between single adsorption and the interface are indicative of a surface dipole change. This change is thus much larger for ethanol than for CCl_4. This supports the idea that the registered strengthening of adsorption at the ethanol/Pt(111) interface is ruled by electrostatic interactions whereas, for CCl_4/Pt(111) system, those interactions should play a minority role.

1.6 Electrostatic potential analysis

Likewise the solid organic platinum interfaces, the average electrostatic potential along the normal to the surface have been plotted for the isolated (010) surfaces of CCl_4 and ethanol crystals. Due to the interaction with platinum, the natural surfaces (PS) exhibiting monoclinic structures, have to distort their morphology in order to fit the hexagonal structure of the metal. The relaxed surfaces after such a lattice distortion are called quasi-surfaces of CCl_4 and ethanol (QS). In Fig. 10 and 11, the electrostatic potentials are drawn for all these systems. Clearly for both organic crystal surfaces, the change of the morphology between monoclinic and hexagonal structures provokes a large dilatation of the organic phase with a strong perturbation of the layering. Hence the decrease of the density of the organic phase in contact with the metal is essentially due to the structural mismatch.

1.7 Charge transfer analysis

The analysis of the charge transfer between the molecule and the platinum surface is addressed in Fig. 12 for both systems. The charge transfer after adsorption is illustrated in presence and in absence of the organic phase. For the dissociated state at the CCl_4/Pt(111) interface, the unusual stabilization of the CCl_3 surface species is elucidated. This weakly adsorbed state results from a clear bonding between $3p_z(Cl_p)$ and various $5d$(Pt) surface states. This bonding is promoted by a depletion in the singly-occupied $2p_x$ orbital of the C atom along the C$-$Cl$_a$ direction. The bonding of the Cl$_a$ at a top site is more classical. For ethanol/Pt(111), the adsorption process is associated with an electronic interaction between $2p_z$(O) and $5d_{z^2}$(Pt) states (dative bond). Clearly, in both situations, the presence of the surrounding organic phase does not affect significantly the chemical bonding between the molecule and the metal.

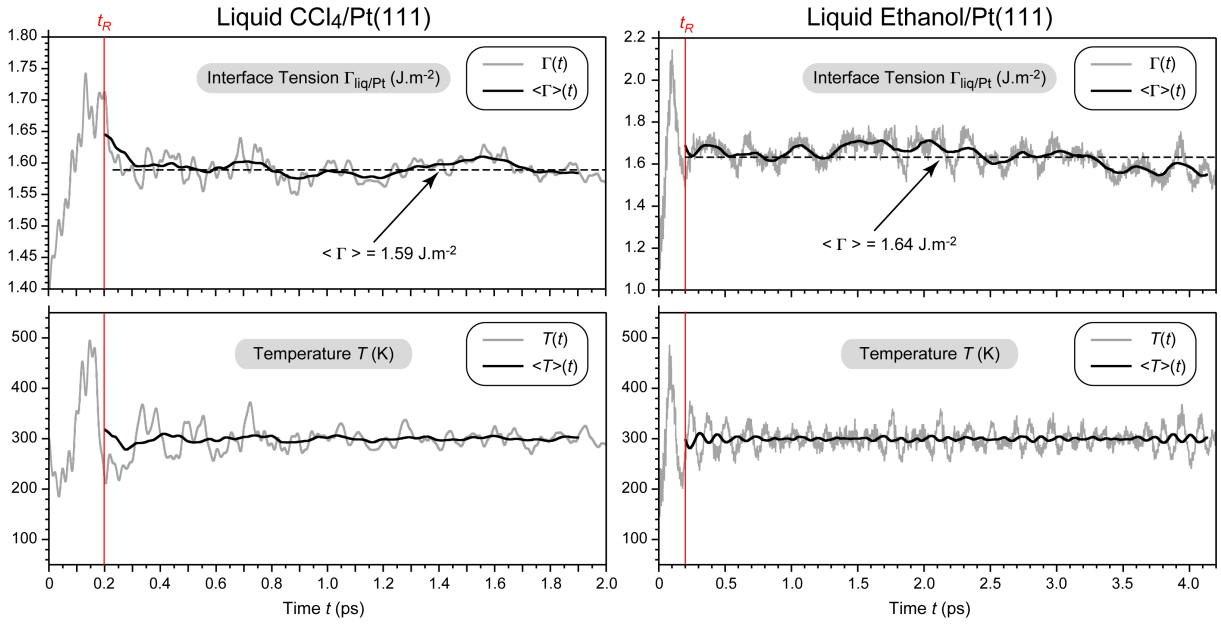

Fig. 13 Time evolution (ps) of the interface tension $\Gamma(t)$ (J.m^{-2}), of the average-by-block interface tension $<\Gamma>(t)$ (J.m^{-2}), of the temperature $T(t)$ (K) and of the average-by-block temperature $<T>(t)$ (K) all along the BOMD simulations (DFT+vdW) at 300 K for the liquid CCl_4/Pt(111) and ethanol/Pt(111) interfaces. The average by block covers over a running constant interval of 0.2 ps. Statistics have been registered after the thermalization step between the chemical systems and Nosé thermostat ($t > t_R = 0.2$ ps). The integration step is 0.5 fs and the characteristic frequency for the Nosé mass is in the range 150-200 cm^{-1}.

2 Liquid Organic-Metal Interfaces

The time evolution of the interface tension and temperature, extracted from Born-Oppenheimer molecular dynamics simulations at 300 K, are exposed in Fig. 13. The corresponding complete movies are available for liquid CCl_4 and ethanol/Pt(111) interfaces. Moreover all along the MD simulations, different snapshots have been taken and presented in Fig. 14 and 15. During the simulation time, two CCl_4 adjacent molecules are dissociated at the liquid CCl_4/Pt(111) interface. For liquid ethanol/Pt(111), several adsorption and desorption processes of ethanol molecules are registered at the platinum surface.

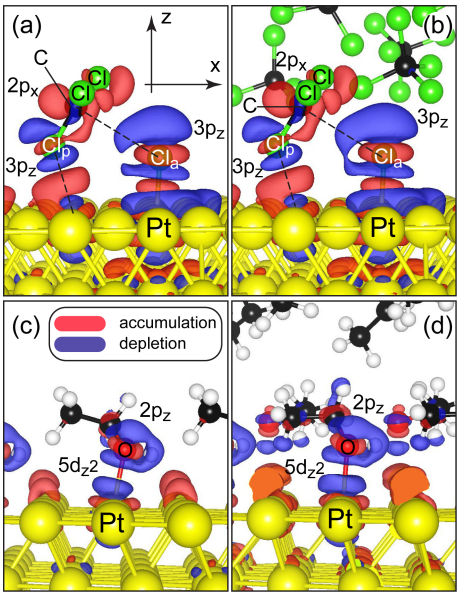

Fig. 12 Charge transfer between the molecule and the platinum surface for (a) single CCl_4 physisorption, (b) the solid CCl_4/Pt(111) interface, (c) single ethanol adsorption and (d) the solid ethanol/Pt(111) interface.

References

1 D. Loffreda, F. Delbecq, D. Simon and P. Sautet, *J. Chem. Phys.*, 2001, **115**, 8101.
2 J. Greeley and M. Mavrikakis, *J. Am. Chem. Soc.*, 2002, **124**, 7193.
3 R. Alcalá, M. Mavrikakis and J. A. Dumesic, *J. Catal.*, 2003, **218**, 178.
4 C. Panja, N. Saliba and B. E. Koel, *Surf. Sci.*, 1998, **395**, 248.
5 K. I. Gursahani, R. Alcalá, R. D. Cortright and J. A. Dumesic, *Applied Catal. A Gen.*, 2001, **222**, 369.
6 G. Mercurio, E. R. McNellis, I. Martin, S. Hagen, F. Leyssner, S. Soubatch, J. Meyer, M. Wolf, P. Tegeder, F. S. Tautz and K. Reuter, *Phys. Rev. Lett.*, 2010, **104**, 036102.

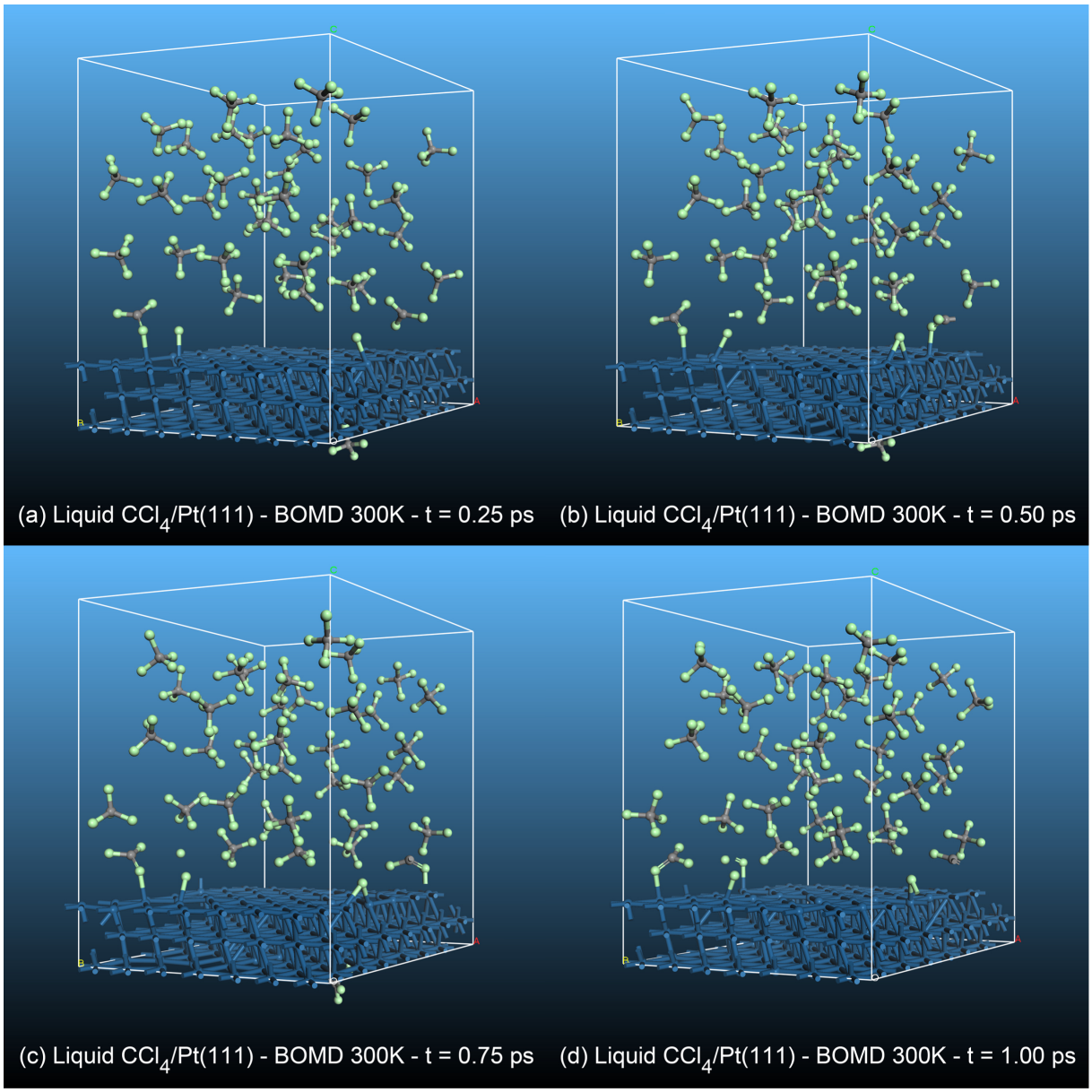

Fig. 14 Stereographic views of the snapshots taken from the molecular dynamics simulation at 300 K for the liquid CCl_4/Pt(111) interface after (a) 0.25 ps, (b) 0.5 ps, (c) 0.75 ps and (d) 1.0 ps. The represented 3D boxes are related to the (7×7) supercell. The interface is composed of 38 CCl_4 molecules and 147 platinum atoms (three metallic layers).

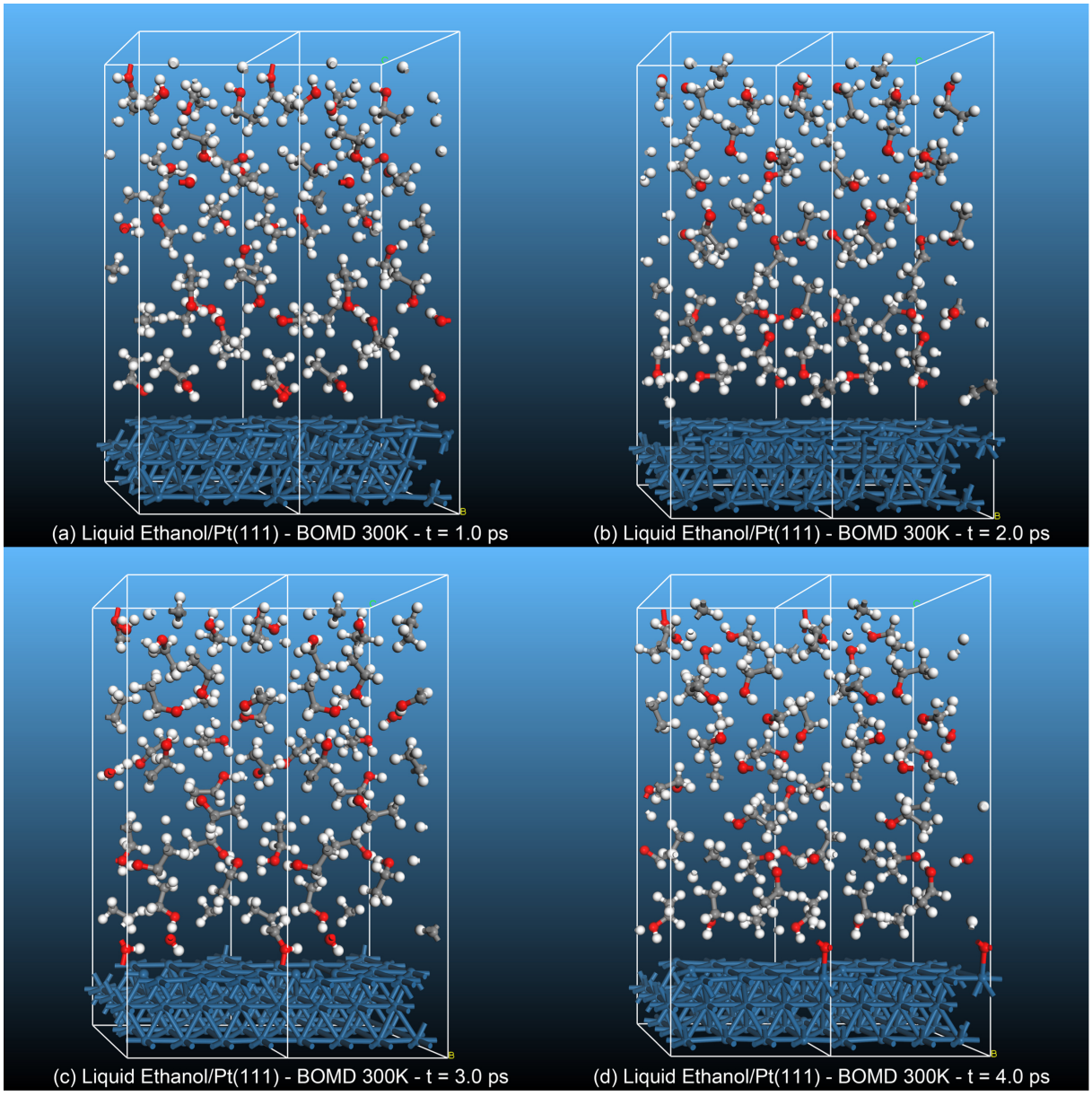

Fig. 15 Stereographic views of the snapshots taken from the molecular dynamics simulation at 300 K for the liquid ethanol/Pt(111) interface after (a) 1.0 ps, (b) 2.0 ps, (c) 3.0 ps and (d) 4.0 ps. The represented 3D boxes are related to the (4×3) supercell. The interface is composed of 21 ethanol molecules and 147 platinum atoms (three metallic layers).